Original Article

Transcriptome sequencing analysis revealed the molecular mechanism of podoplanin neutralization inhibiting ischemia/reperfusion-induced microglial activation

Shuang Qian[1,2#]^, Lei Qian[3#], Ye Yang[1,2]^, Jie Cui[1,2]^, Yiming Zhao[1,2]^

[1]Jiangsu Institute of Hematology, Key Laboratory of Thrombosis and Hemostasis of the Ministry of Health, The First Affiliated Hospital of Soochow University, Suzhou, China; [2]Collaborative Innovation Center of Hematology, Soochow University, Suzhou, China; [3]Department of Clinical Laboratory, Binhai County People's Hospital, Binhai, China

Contributions: (I) Conception and design: S Qian; (II) Administrative support: Y Zhao; (III) Provision of study materials or patients: Y Zhao; (IV) Collection and assembly of data: S Qian; (V) Data analysis and interpretation: L Qian; (VI) Manuscript writing: All authors; (VII) Final approval of manuscript: All authors.

[#]These authors contributed equally to this work and should be considered as co-first authors.

Correspondence to: Yiming Zhao. Jiangsu Institute of Hematology, Key Laboratory of Thrombosis and Hemostasis of the Ministry of Health, The First Affiliated Hospital of Soochow University, 188 Shizi Street, Suzhou 215006, China. Email: zhaoyimingbox@163.com.

Background: Anti-podoplanin antibody (α-PDPN, clone 8.1.1) reduces microglia-mediated inflammation and decreases cerebral infarct volume in mice with stroke. However, the molecular mechanism by which this occurs is unknown. This study sought to systematically analyze the molecular mechanism of α-PDPN treatment on ischemia/reperfusion (I/R)-injured microglia.

Methods: Microglia BV2 cells were pre-cultured with α-PDPN and then exposed to oxygen-glucose deprivation and reoxygenation (OGD-R) insult. The differentially expressed genes (DEGs) underwent a transcriptome sequencing technology analysis, followed by Gene Ontology (GO) and Kyoto Encyclopedia of Genes and Genomes (KEGG) pathway enrichment analyses. Quantitative real-time polymerase chain reaction (PCR) was performed to confirm the transcriptional expression of some DEGs.

Results: The results showed that α-PDPN downregulated 338 genes and upregulated 340 genes in the BV2 cells. The GO items of the downregulated DEGs mainly involved biological processes, such as the response to the interferon (IFN), lipopolysaccharide-mediated signaling pathway, and the regulation of cell chemotaxis and migration. The upregulated molecular function mainly involved glucocorticoid-receptor binding. Further, the KEGG pathway analysis indicated that the enriched categories for the upregulated DEGs mainly involved the adenosine triphosphate (ATP) binding cassette transporters. However, the interleukin-17 signaling pathway, IFN signaling pathway, tumor necrosis factor signaling pathway, transforming growth factor beta (TGF-β) signaling pathway, nucleotide-binding and oligomerization domain (NOD)-like receptor signaling pathway, cytokine-cytokine receptor interaction, and chemokine signaling pathway were downregulated by the α-PDPN treatment.

Conclusions: Numerous inflammation-related signaling pathways were regulated by the α-PDPN treatment in the OGD-R injured BV2 cells. This study provided further insights into the protective mechanism of α-PDPN treatment in ischemic stroke.

Keywords: Podoplanin; ischemic stroke; transcriptome sequencing; microglia

Submitted Mar 28, 2022. Accepted for publication May 10, 2022.
doi: 10.21037/atm-22-1952
View this article at: https://dx.doi.org/10.21037/atm-22-1952

^ ORCID: Shuang Qian, 0000-0003-2888-5544; Yiming Zhao, 0000-0002-6960-9370; Ye Yang, 0000-0001-6944-8004; Jie Cui, 0000-0001-5488-3951.

Introduction

Acute ischemic stroke (IS) is a leading cause of disability and death in adults worldwide, especially in China, where there are >2 million new cases per year (1,2). Neuroinflammation, which occurs minutes to hours after stroke, is a major pathological process and is significantly associated with brain damage (3). Numerous animal and clinical studies have suggested that the inflammatory modulation of the central nervous system might be a viable alternative therapeutic strategy for acute IS (3,4).

Microglia are resident innate immune cells in the brain and play crucial roles in both pathological and physiological conditions, such as response to brain injury, microenvironment maintenance, and pathogen defense (5,6). After the occurrence of cerebral ischemia, microglia are mobilized and transferred to the damaged areas, where they rapidly release cytotoxic mediators and contribute to the occurrence and spread of neuroinflammation (7). Cerebral reperfusion further activates microglia and leads to an enhanced cascade of inflammatory responses that ultimately lead to further neuronal damage, which is referred to as ischemia/reperfusion injury (I/R) (8). Currently, few ideal drugs are available to suppress microglia-mediated inflammation (9).

Podoplanin (PDPN), which is a small transmembrane mucin-like glycoprotein, is widely expressed in microglia, dendritic cells, type I alveolar cells, macrophages, and different types of fibroblasts (10). Previous studies have shown that PDPN promotes the inflammatory response in different diseases, including rheumatoid arthritis, lung injury, and traumatic brain injury (10,11). Additionally, the neutralization of PDPN via an anti-PDPN antibody (α-PDPN) has been shown to suppress inflammatory responses and improve heart function after myocardial infarction (12). Recently, the role of PDPN in neuroinflammation has been examined. PDPN expression can be induced by hydrogen peroxide, lipopolysaccharide, hemoglobin, and I/R injury on microglia, and play a pro-inflammatory role in cerebral injury (13,14). Notably, α-PDPN pretreatment has been shown to attenuate neurological deficits and reduce cerebral infarct volume in a mouse model of IS by reducing the inflammatory response (14). However, the molecular mechanism by which α-PDPN inhibits I/R-induced microglial activation is not fully understood.

Thus, this study sought to explore the molecular mechanism by which α-PDPN inhibits the activation of microglia subjected to I/R injury. In this study, microglia BV2 cells were pre-treated with α-PDPN and then subjected to oxygen-glucose deprivation and reoxygenation (OGD-R). The differentially expressed genes (DEGs) underwent a transcriptome sequencing technology analysis, followed by Gene Ontology (GO) and Kyoto Encyclopedia of Genes and Genomes (KEGG) pathway enrichment analyses. The RNA-seq data are available in GenBank Sequence Read Archive (SRA) database with accession number PRJNA825112. We present the following article in accordance with the MDAR reporting checklist (available at https://atm.amegroups.com/article/view/10.21037/atm-22-1952/rc).

Methods

α-PDPN treatment and OGD-R insult

The murine microglial BV2 cell line (5×10^4 cells/mL, Procell Life Science and Technology, Co. Ltd., Wuhan, China) was cultured in complete Dulbecco's Modified Eagle's medium (DMEM, Procell Life Science and Technology, Co. Ltd.) containing 10% fetal bovine serum, streptomycin (100 U/mL), and penicillin (100 U/mL) at 37 ℃ with 5% carbon dioxide (CO_2). Next, the cells were treated with α-PDPN (10 μg/mL, Bio X Cell, clone 8.1.1, West Lebanon, NH, USA) in complete DMEM medium for 6 h, and then subjected to OGD-R, which is an accepted *in-vitro* model of I/R (15). In brief, the cells were grown in a serum and glucose-free medium in a hypoxia chamber (H35; Don Whitley Scientific Ltd., Shipley, UK) containing 5% CO_2 and 95% nitrogen at 37 ℃ for 6 hours. The cells were then grown in complete DMEM medium for 20 h in an incubator with 5% CO_2 and 95% air at 37 ℃. The cells in the α-PDPN group were treated with α-PDPN (10 μg/mL) during OGD-R (n=3 per group), and the cells in the control group were treated with phosphate buffered solution (20 μL, 0.01 M, pH 7.4).

Transcriptome sequencing analysis

Total ribonucleic acid (RNA) was extracted from the BV2 cells, and its quality was detected. Briefly, total RNA was extracted using a RNeasy mini kit (Qiagen, Duesseldorf, Germany). Qualified total RNA (3 μg) was further purified by an RNA Clean XP Kit (Cat A63987, Beckman Coulter, Inc. Kraemer Boulevard Brea, CA, USA). An RNA library was generated using the RNA-Sequencing Library Prep Kit (Illumina, CA, USA) in accordance with the manufacturer's

instructions. First, total RNA was cut into short fragments by a fragment high mix buffer at 94 ℃ for 8 min. Next, the 1st-strand complementary deoxyribonucleic acid (cDNA) was synthesized at 25 ℃ for 10 min, followed by 42 ℃ for 15 min, and 70 ℃ for 15 min. The 2nd-strand cDNA was subsequently synthesized at 16 ℃ for 1 h. The cDNA fragments were then treated with A-Tailing Mix, and the adapters were ligated to the ends of these template DNAs. Finally, the cDNA library was synthesized by polymerase chain reaction (PCR) amplification, and library quality was evaluated on an Agilent 2100 BioAnalyzer (Agilent Technologies, Santa Clara, CA, USA). The RNA library was run on a NovaSeq 6000 platform (Illumina, CA, USA). The library construction and sequence analysis were performed at Shanghai Boho Biological Co. Ltd. (Shanghai, China).

Screening of DEGs

To normalize the expression levels of different genes and different samples, the reads were converted to fragments per kilobase of transcripts per million fragments mapped (FPKM) value. The false discovery rate (FDR) is the adjusted P value obtained by multiple hypothesis test correction on the original P value (16). The DEGs in the libraries were defined as having a FPKM value ≥1.5 and an FDR <0.05.

Functional annotation of the DEGs

To better understand the biological functions and pathways associated with the DEGs, GO and KEGG enrichment analyses were performed using the functional annotation tool of Database for Annotation, Visualization, and Integrated Discovery (DAVID) (version 6.8, https://david.ncifcrf.gov). The number of DEGs contained in each GO item and the rich factor of each GO item was calculated. A GO item with a P value <0.05 was considered significantly enriched. Additionally, a KEGG pathway analysis was conducted to harvest pathway clusters and describe the molecular interactions in differentially genes. In the pathway map, the DEGs were marked red if upregulated and green if downregulated.

Real-time polymerase chain reaction (RT-PCR) confirmation

The expression of 9 DEGs was selected and validated by RT-PCR. Among them, the following 6 genes were downregulated: interferon regulatory factor 7 (*IRF7*), interferon-gamma inducible protein 204 (*IFI204*), interferon-stimulated gene 20 (*ISG20*), *ISG15*, chemokine (C-C motif) ligand 2 (*CCL2*), and *CCL7*. Among them, the following 3 genes were upregulated: nuclear receptor subfamily 4 group A member 1 (*Nr4a1*), ATP Binding cassette subfamily A member 5 (*Abca5*), and cyclin B2 (*CCNB2*). Total RNA was isolated using Trizol (Invitrogen, Carlsbad, CA, USA). Next, the mRNA was reversely transcribed to cDNA. Subsequently, RT-PCR was performed using the SYBR-Green PCR Master Mix kit (Takara, Tokyo, Japan) at 55 ℃ for 2 min, followed by 35 cycles of 95 ℃ for 20 s and 60 ℃ for 1 min on a PCR Detection System (Applied Biosystems, Prism 7500, USA). All RT-PCR reactions were performed 3 times. The $2^{-\Delta\Delta Ct}$ method was used to calculate the relative quantification with calibration to the internal control glyceraldehyde-3-phosphate dehydrogenase (GAPDH). The specific primers for the selected genes are listed in *Table 1*.

Statistical analysis

For the sequencing data, the FDR value was P<0.05 or a difference multiple ≥2 between the 2 groups indicated statistical significance. For the RT-PCR, the data are expressed as the mean ± standard error of the mean (SEM). The statistical analysis was performed using GraphPad Prism version 5.0 (GraphPad Software Inc., San Diego, CA, USA).

Results

Identification of DEGs

A principal component analysis (PCA) is a statistical technique for dimensionality reduction. Using a covariance or correlation matrix, the PCA performs a linear transformation, replacing possibly related variables with a set of smaller linear independent variables (17). In this study, the score plots of the PCA showed an obvious separation between the α-PDPN (PC1, 60.6%) and OGD-R (PC2, 11.9%) groups (see *Figure 1A*). A larger PC1 value indicated a larger degree of genetic change by α-PDPN treatment.

Further, 338 mRNAs were downregulated and 340 mRNAs were upregulated in the α-PDPN treatment group as compared to OGD-R group (fold change ≥2; q<0.05; see *Figure 1B*). The top 40 downregulated and upregulated genes are shown in *Figure 1C*,*1D*, respectively. Several

Table 1 Sequences of the specific primers for PCR confirmation

Gene name	Forward primer (5'–3')	Reverse primer (5'–3')
IRF7	CCCCAGCCGGTGATCTTTC	CACAGTGACGGTCCTCGAAG
IFI204	CAGGGAAAATGGAAGTGGTG	CAGAGAGGTTCTCCCGACTG
ISG20	AACATC CAG AACAACTGG CGG	GTCTGACGTCCCAGGGCA
ISG15	TCCATGACGGTGTCAGAACT	GACCCAGACTGGAAAGGGTA
CCL2	CCACTCACCTGCTGCTACTCATTC	CTGCTGCTGGTGATCCTCTTGTAG
CCL7	TCAAGAGCTACAGAAGGATCACC	TGGAGTTGGGGTTTTCATGTCT
Abca5	ATTCTTGGATACACTCCCGTGA	ACCTTGGGAAGATGATCGGTA
CCNB2	TCTACCAGTACCTCAGGCAGCTTG	CACCAGGATGGCACGCATACG
Nr4a1	AGTTGGGGGAGTGTGCTAGA	GCTTGAATACAGGGCATCTCCAG
GAPDH	AGGTCGGTGTGAACGGATTTG	TGTAGACCATGTAGTTGAGGTCA

IRF7, interferon regulatory factor 7; IFI204, interferon-gamma inducible protein 204; ISG20, interferon-stimulated gene 20; CCL2, chemokine (C-C motif) ligand 2; Abca5, ATP Binding cassette subfamily A member 5; CCNB2, cyclin B2; Nr4a1, nuclear receptor subfamily 4 group A member 1; GAPDH, glyceraldehyde-3-phosphate dehydrogenase.

downregulated genes were related to interferon (IFN) regulators and chemokines, such as *IRF7*, *ISG20*, *ISG15*, *IFI204*, *CCL2*, *CCL7*, and *CCL12*.

Verification of DEGs by RT-PCR

To validate the DEGs identified by the RNA-sequencing platform, 9 DEGs were selected for the RT-PCR confirmation. In line with the results of the transcriptome sequencing analysis, the RT-PCR results indicated that the gene expression of *IRF7*, *IFI204*, *ISG20*, *ISG15*, *CCL2*, and *CCL7* was more reduced, and the gene expression of *Nr4a1*, *Abca5*, and *CCNB2* was more increased in the BV2 cells in the α-PDPN treatment group than the OGD-R group (fold change ≥2; P<0.05; see *Figure 2A-2I*). Thus, the results of the transcriptome sequencing analysis were largely consistent with those of the RT-PCR analysis, which provides some evidence of the credibility of the transcriptome sequencing data.

GO functional enrichment analysis

To detect the biological functions of the identified DEGs, a GO functional enrichment analysis was conducted. The top 30 enriched categories of the downregulated DEGs in the BV2 cells after the α-PDPN treatment are shown in *Figure 3A*. The downregulated GO terms mainly involved biological processes, such as response to IFNs (IFN-α, and IFN-β), progesterone, the lipopolysaccharide-mediated signaling pathway, viral genome replication, and the regulation of cell chemotaxis (including macrophages, eosinophils, monocytes, granulocytes, and lymphocytes), and migration (including mononuclear cells, eosinophils, and lymphocytes). The downregulated molecular function was enriched in C-C motif chemokine receptor (CCR) binding. The upregulated expressed GO terms are shown in *Figure 3B*. The upregulated molecular functions mainly involved glucocorticoid receptor (GR) binding. These results indicate that the α-PDPN treatment inhibited IFN signaling and cell chemotaxis and migration, but upregulated GR binding in the I/R-injured BV2 cells.

KEGG pathway enrichment analysis

A KEGG pathway analysis of the DEGs was conducted. The top 30 rich factors of the downregulated pathways are shown in *Figure 4A*. The enriched categories of the upregulated DEGs mainly involved the ATP-binding cassette (ABC) transporters (see *Figure 4B*). As *Table 2* shows, the downregulated pathways included the IL-17 signaling pathway, osteoclast differentiation, hepatitis C, influenza A, the tumor necrosis factor (TNF) signaling pathway, Epstein-Barr virus infection, the chemokine signaling pathway, the transforming growth factor beta (TGF-β) signaling pathway, the nucleotide-binding and oligomerization domain (NOD)-like receptor (NLR)

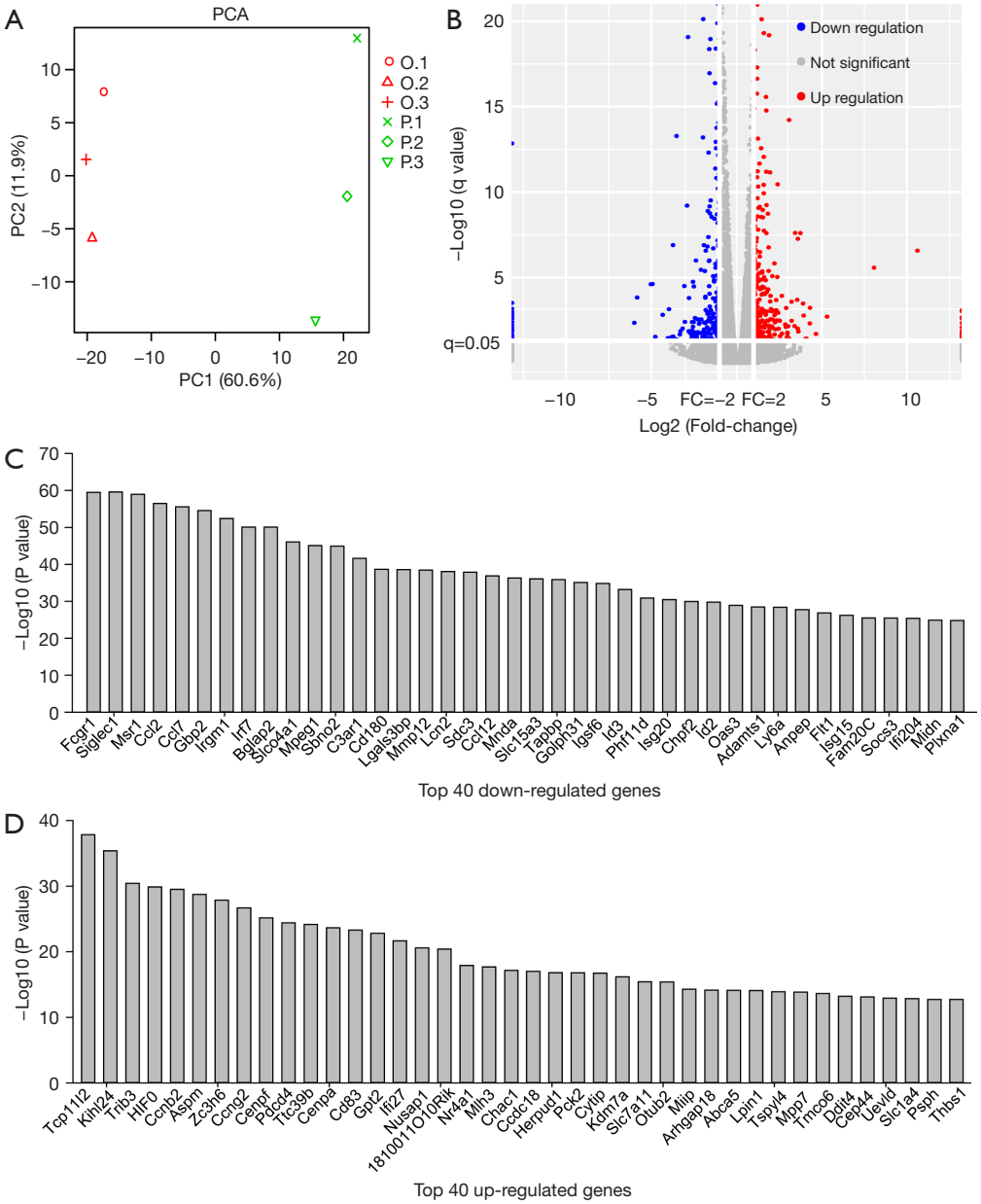

Figure 1 Gene expression changes induced by α-PDPN treatment in the BV2 cells. The microglia were pre-treated with α-PDPN (10 μg/mL) for 6 h and then subjected to 6 h OGD and 24 h reoxygenation, after which a transcriptome sequencing analysis was conducted. (A) The score plots of the PCA showed an obvious genetic change by the α-PDPN treatment. α-PDPN + OGD-R *vs.* OGD-R (PC1 and PC2). (B) The DEGs between the 2 groups are shown in a volcano plot. The q-value is the adjusted p-value using multiple hypothesis testing. (C) The top 40 down-regulated DEGs by the α-PDPN treatment. (D) The top 40 up-regulated DEGs by the α-PDPN treatment. PCA, principal component analysis; α-PDPN, anti-podoplanin antibody; OGD, oxygen-glucose deprivation; OGD-R, oxygen-glucose deprivation and reoxygenation; DEGs, differentially expressed genes.

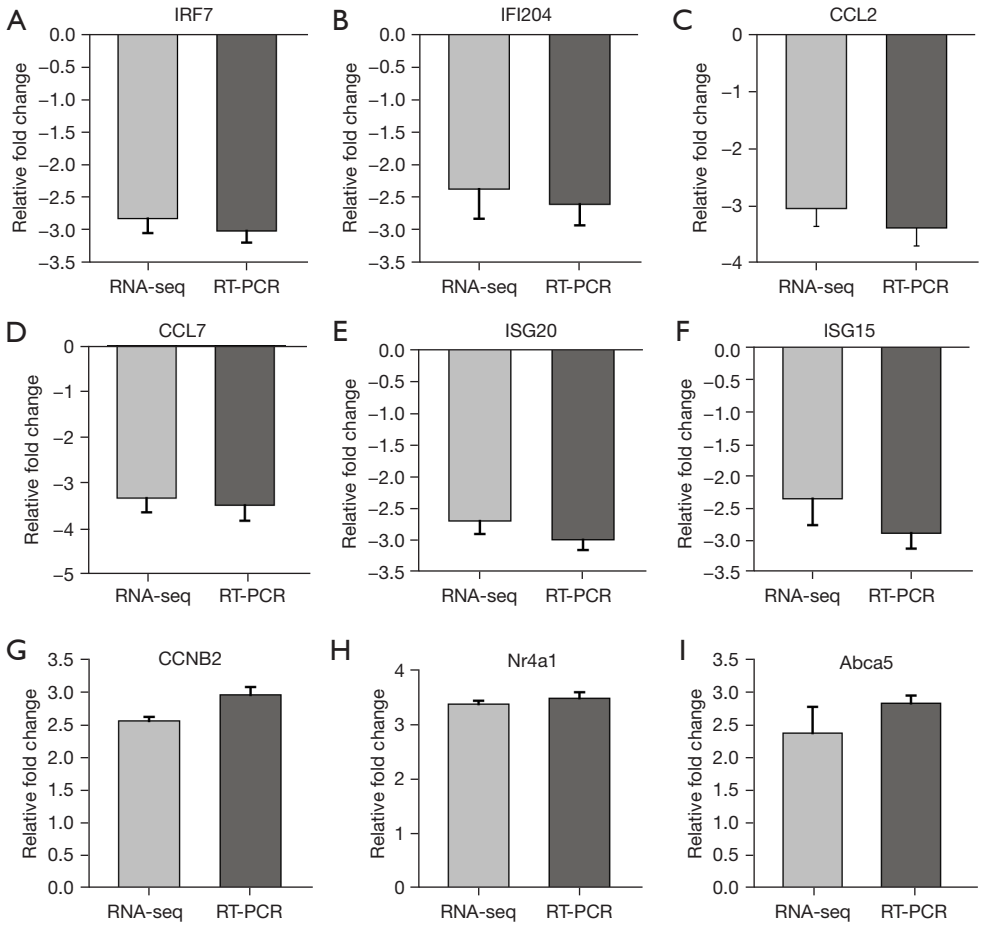

Figure 2 Validation of the RNA-sequencing data by RT-PCR. The microglia were pre-treated with α-PDPN (10 μg/mL) for 6 h and then subjected to 6 h oxygen-glucose deprivation and 24 h reoxygenation, after which RT-PCR was conducted. (A-I) The results of the transcriptome sequencing analysis for the 9 identified genes were largely consistent with those of the RT-PCR analysis. Error bars represent the mean ± SD of three independent experiments. RT-PCR, real-time polymerase chain reaction; α-PDPN, anti-podoplanin antibody; IRF7, interferon regulatory factor 7; IFI204, interferon-gamma inducible protein 204; ISG20, interferon-stimulated gene 20; CCL2, chemokine (C-C motif) ligand 2; Nr4a1, nuclear receptor subfamily 4 group A member 1; Abca5, ATP binding cassette subfamily A member 5; CCNB2, cyclin B2.

signaling pathway, and cytokine-cytokine receptor interaction (rich factor >3, Q value <0.05).

The genes involved in the hepatitis C signaling pathway were significantly downregulated in the BV2 cells after the α-PDPN treatment (see *Table 2*). Similarly, the α-PDPN treatment suppressed the IFN-related pathways, such as influenza A, Epstein-Barr virus infection, and measles (see *Table 2*). Additionally, many genes involved in the IL-17 signaling pathway were downregulated, such as IL-17A receptor (*IL-17RA*), activator protein-1, S100 calcium binding proteins A8 (*S100A8*), matrix metallopeptidase-13 (*MMP13*), *CCL7*, *CCL2*, and lipocalin 2 (*LCN2*) (see *Table 2*). Further, the KEGG pathway analysis indicated that many genes involved in the NLR signaling pathway were downregulated, such as *IRF3/7*, *IFI16/IFI204*, guanylate-binding protein 2 (*Gbp2*), signal transducer and activator of transcription 2 (*Stat2*), 2'-5'-oligoadenylate synthetase 3 (*Oas3*), monocyte chemoattractant protein-1 (*MCP-1*, also known as *CCL2*), and chemokine RANTES (also known as *CCL5*) (see *Table 2*). These results suggested that the α-PDPN treatment inhibited the inflammatory response in the OGD-R injured microglia.

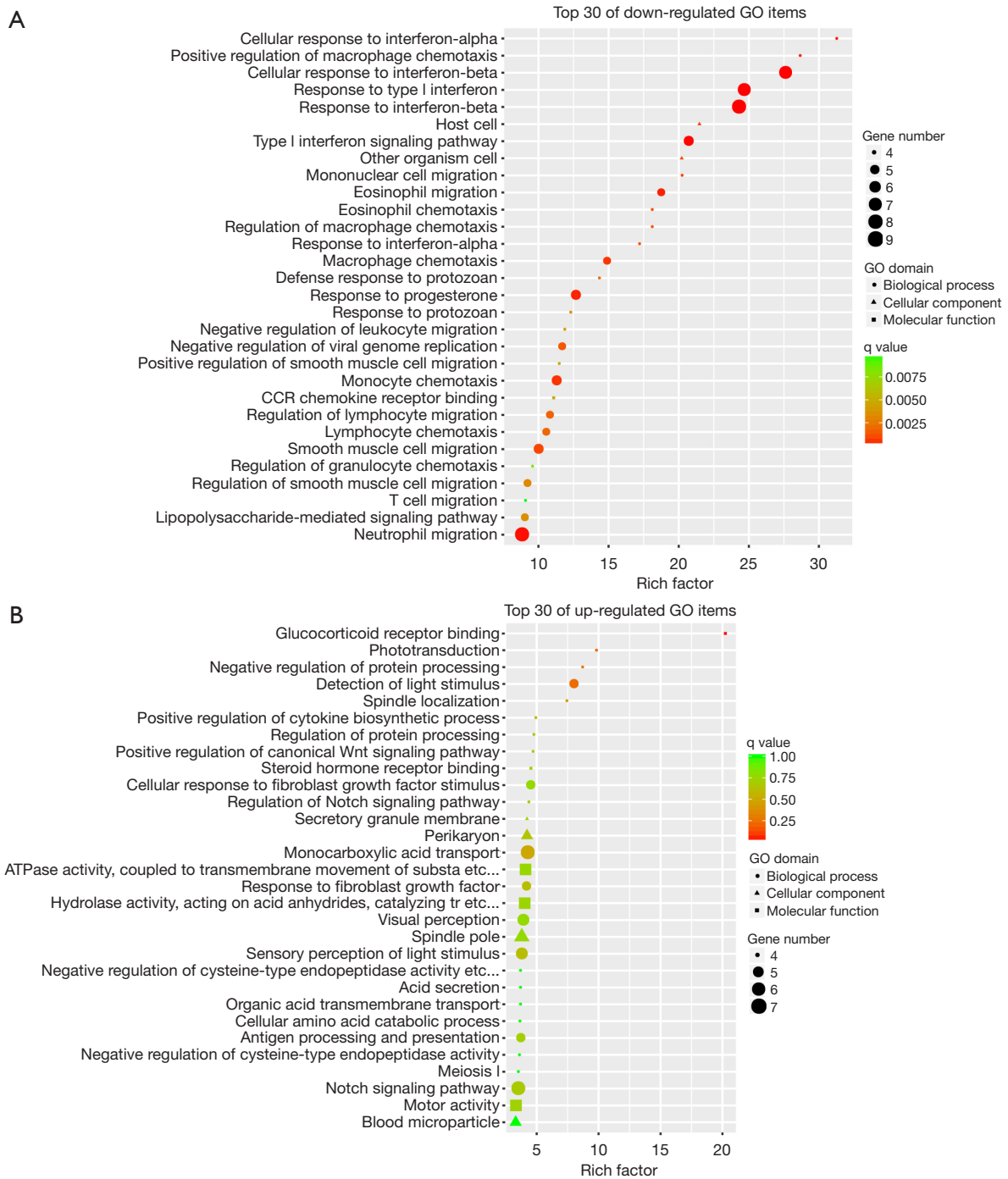

Figure 3 The top 30 terms in the GO analysis of the DEGs in the BV2 cells after treatment with α-PDPN. The microglia were pre-treated with α-PDPN (10 μg/mL) for 6 h and then subjected to 6 h OGD and 24 h reoxygenation, after which a transcriptome sequencing analysis was conducted. After the DEGs were identified, the GO functional enrichment analysis was conducted. (A) The top 30 down-regulated GO terms of DEGs. (B) The top 30 up-regulated GO terms of DEGs. CCR, C-C motif chemokine receptor; GO, Gene Ontology; DEGs, differentially expressed genes; α-PDPN, anti-podoplanin antibody; OGD, oxygen-glucose deprivation.

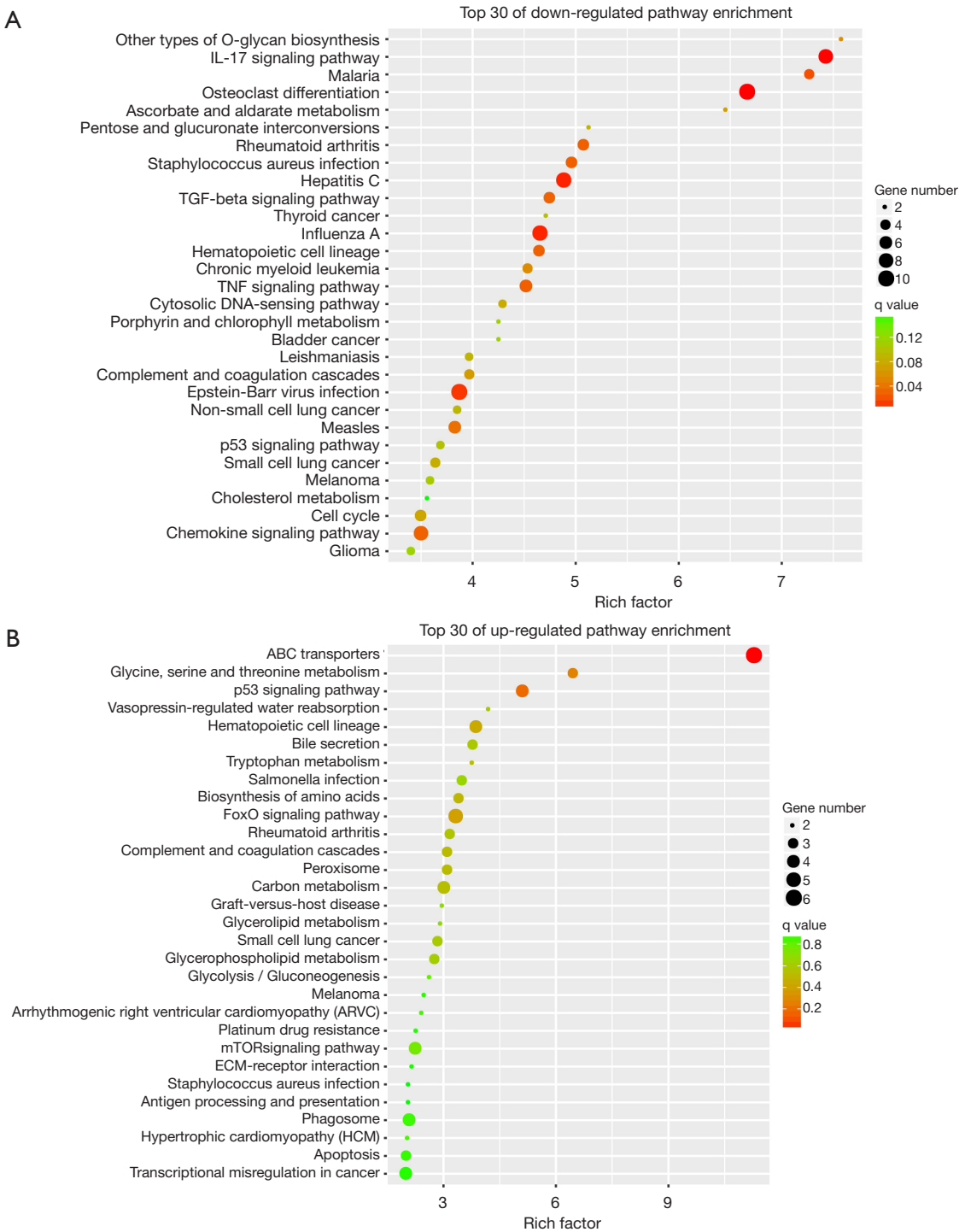

Figure 4 The top 30 pathways in the KEGG analysis of the DEGs in the BV2 cells after treatment with α-PDPN. The microglia were pre-treated with α-PDPN (10 μg/mL) for 6 h and then subjected to 6 h oxygen-glucose deprivation and 24 h reoxygenation, after which a transcriptome sequencing analysis was conducted. After the DEGs were identified, the KEGG pathway enrichment analysis was conducted. (A) The top 30 down-regulated KEGG pathways of DEGs. (B) The top 30 up-regulated KEGG pathways of DEGs. IL-17, interleukin-17; TGF, tumor necrosis factor; TNF, tumor necrosis factor; ECM, extracellular matrix; KEGG, Kyoto Encyclopedia of Genes and Genomes; DEGs, differentially expressed genes; α-PDPN, anti-podoplanin antibody.

Table 2 KEGG analysis of the DEGs in the BV2 cells after treatment with α-PDPN

Pathway ID	Pathway description	Gene down list	Rich factor	P value	Q value
mmu04657	IL-17 signaling pathway	*S100a8, Mmp13, Fosl1, Il17ra, Ccl7, Ccl12, Ccl2, Lcn2*	7.408642	5.97E-06	0.000543
mmu05144	Malaria	*Tgfb1, Lrp1, Ccl12, Ccl2*	7.254296	0.00061	0.018499
mmu04380	Osteoclast differentiation	*Gm15931, Tgfb1, Socs3, Fosl1, Sirpb1a, Stat2, Fcgr4, Fcgr1, Junb, Pirb*	6.645156	1.87E-06	0.000341
mmu05323	Rheumatoid arthritis	*Flt1, Tgfb1, Ccl5, Ccl12, Ccl2*	5.061136	0.001304	0.026374
mmu05150	Staphylococcus aureus infection	*C3ar1, Cfb, Fcgr4, C5ar1, Fcgr1*	4.946111	0.001467	0.026695
mmu05160	Hepatitis C	*Irf7, Myc, Ifit1bl1, Socs3, Stat2, E2f2, Oas3, Ifit1, Mx2*	4.866236	7.08E-05	0.004298
mmu04350	TGF-beta signaling pathway	*Myc, Tgfb1, Id3, Id1, Id2*	4.731062	0.001838	0.02788
mmu05164	Influenza A	*Irf7, Ccl5, Socs3, Stat2, Oas3, Ccl12, Ccl2, Tnfsf10, Mx2*	4.635881	0.000105	0.004786
mmu04640	Hematopoietic cell lineage	*Anpep, Itga5, Csf2ra, Cd34, Fcgr1*	4.630401	0.002049	0.026638
mmu05220	Chronic myeloid leukemia	*Myc, Tgfb1, E2f2, Gadd45g*	4.522158	0.004861	0.05529
mmu04668	TNF signaling pathway	*Ccl5, Socs3, Junb, Bcl3, Ccl12, Ccl2*	4.502666	0.001134	0.025797
mmu05169	Epstein-Barr virus infection	*Irf7, H2-T24, Myc, Isg15, Stat2, E2f2, Oas3, Gadd45g, Jak3, Tapbp*	3.851838	0.000255	0.009279
mmu05162	Measles	*Irf7, Stat2, Oas3, Jak3, Tnfsf10, Mx2*	3.812476	0.002916	0.035386
mmu04062	Chemokine signaling pathway	*Ccr4, Ccl5, Stat2, Ccl7, Jak3, Cxcr3, Ccl12, Ccl2*	3.482062	0.00166	0.027458
mmu04621	NOD-like receptor signaling pathway	*Irf7, Gbp2, Ccl5, Stat2, Oas3, Ccl12, Ccl2, Ifi204*	3.380643	0.002029	0.028403
mmu04060	Cytokine-cytokine receptor interaction	*Ccr4, Tgfb1, Csf2ra, Ccl5, Il17ra, Ccl7, Tnfsf12, Cxcr3, Ccl12, Ccl2, Tnfsf10*	3.202565	0.000739	0.019208

KEGG, Kyoto Encyclopedia of Genes and Genomes; DEGs, differentially expressed genes; α-PDPN, anti-podoplanin antibody; IL-17, interleukin-17; TGF, transforming growth factor; TNF, tumor necrosis factor; NOD, nucleotide-binding and oligomerization domain.

Discussion

The molecular mechanism of α-PDPN treatment on I/R-injured microglia remains unclear. In this study, we used OGD-R injured BV2 cells to explore changes in the transcriptome sequencing data after the α-PDPN treatment. The results indicated that a total of 338 genes were downregulated and 340 genes were upregulated in the α-PDPN-treated BV2 cells. Notably, the GO and KEGG enrichment analyses revealed that the α-PDPN treatment inhibited the inflammation-related signaling pathways in the OGD-R injured microglia.

It is widely known that the activation of the type-I IFN pathway in microglia is detrimental to the prognosis of IS, as it creates a pro-inflammatory environment (18,19). Hypoxia and ischemia can directly induce microglial activation, and numerous interferon-stimulated genes (ISG) have been shown to be increased in brain tissue subjected to I/R, which in turn activates the type-I IFN pathway, leading to neuroinflammation (20). Recently, Liao *et al.* proposed that the cyclic GMP-AMP synthase (cGAS) is activated in the ischemic penumbra of mice by self-mitochondrial DNA released from the mitochondria of cells, which in turn promotes the activation of the IFN signaling pathway (21). In the current study, we found that several GO items involved in the IFN signaling pathway were downregulated after

the α-PDPN treatment. Similar results were found in the KEGG enrichment analysis, and the α-PDPN treatment suppressed a number of IFN signaling pathways, such as the hepatitis C, influenza A, and Epstein-Barr virus infection pathways.

The GO enrichment analysis revealed that the α-PDPN treatment inhibited the chemotaxis and migration of a variety of cells, including eosinophils, lymphocytes, macrophages, monocytes, and granulocytes. In the presence of tissue damage, microglia are polarized toward the pro-inflammatory M1 phenotype, releasing pro-inflammatory chemokines such as CCl2, CCL12, and CCL7, which guide other immune cells to migrate to the damaged area and initiate an inflammatory response (22). Consistent with these findings, the KEGG enrichment analysis showed that the α-PDPN treatment inhibited the IL-17 signaling pathway. The binding of IL-17 to the IL-17R activates the IL-17R signaling pathway and ultimately triggers the expression of proinflammatory chemokines (CCL2, CCL7, and CCL20) (23). Similarly, the effect of α-PDPN on IL-17 signaling pathway was reported in an *in-vitro* experimental study, which showed that the preincubation of isolated peripheral blood mononuclear cells with α-PDPN reduced the secretion of IL-17 and IL-1β (24).

Our study also showed that the α-PDPN treatment increased GR binding and ABC transporters in I/R-injured BV2 cells. Ligand-occupied GRs have powerful anti-inflammatory effects, which act by repressing or inducing the transcription of target genes by direct binding to DNA response elements and/or by other transcription factors (25). For example, nuclear receptor 4a1 (Nr4a1), a member of GRs, has been identified as a key rheostat that controls microglial activation and pro-inflammatory polarization (26,27). Notably, we demonstrated that the α-PDPN treatment increased the Nr4a1 expression in the BV2 cells. Consistently, Gibson *et al.* reported that ABC transporters inhibit the inflammatory response of microglia, and that the decreased function of ABC transporters leads to the retention of toxic chemicals and abnormal cell-cell communication (28).

Further, it is increasingly accepted that the NLR signaling pathways have a detrimental effect on the progression of IS. For example, the NLR protein 3 (NLRP3) inflammasome drives robust inflammation and pyroptosis (lytic cell death) in neurological diseases such as ischemic brain injury (29). Recently, several research groups have shown that the IFN signaling pathways play an important role in the activation of the NLR signaling pathways. For example, Li *et al.* reported that phosphorylated IRF3 translocated into the nucleus and increased the expression of NLRP3 in a mouse cardiomyocytes model (30). Additionally, IFI204 and its human homologue IFI16 are involved in the detection of aberrant nucleic acid, originating from mitochondrial or DNA damage. The elevated expression of IFI16/IFI204 initiates the activation of the cGAS/stimulator of interferon genes (STING) (a stimulator of IFN genes) pathway, which in turn promotes the activation of the NLR signaling pathways (31,32). Our study showed that the α-PDPN treatment decreased the expression of IRF7, ISG15, and IFI204 in BV2 cells.

In conclusion, there were a large number of DEGs in the OGD-R injured BV2 cells after the α-PDPN treatment. The GO and KEGG enrichment analyses showed that the α-PDPN treatment mainly inhibited the expression of inflammation-related genes and signaling pathways. Our findings not only provide insights into the molecular regulation mechanism of α-PDPN treatment, but also provide a basis for extending its use in clinical trials.

Acknowledgments

Funding: This work was supported by the National Natural Science Foundation of China (No. 81873431).

Footnote

Reporting Checklist: The authors have completed the MDAR reporting checklist. Available at https://atm.amegroups.com/article/view/10.21037/atm-22-1952/rc

Data Sharing Statement: Available at https://atm.amegroups.com/article/view/10.21037/atm-22-1952/dss

Conflicts of Interest: All authors have completed the ICMJE uniform disclosure form (available at https://atm.amegroups.com/article/view/10.21037/atm-22-1952/coif). The authors have no conflicts of interest to declare.

Ethical Statement: The authors are accountable for all aspects of the work in ensuring that questions related to the accuracy or integrity of any part of the work are appropriately investigated and resolved.

References

1. GBD 2017 Causes of Death Collaborators. Global, regional, and national age-sex-specific mortality for 282 causes of death in 195 countries and territories, 1980-2017: a systematic analysis for the Global Burden of Disease Study 2017. Lancet 2018;392:1736-88.
2. Wu S, Wu B, Liu M, et al. Stroke in China: advances and challenges in epidemiology, prevention, and management. Lancet Neurol 2019;18:394-405.
3. Maida CD, Norrito RL, Daidone M, et al. Neuroinflammatory Mechanisms in Ischemic Stroke: Focus on Cardioembolic Stroke, Background, and Therapeutic Approaches. Int J Mol Sci 2020;21:6454.
4. Han B, Jiang W, Cui P, et al. Microglial PGC-1α protects against ischemic brain injury by suppressing neuroinflammation. Genome Med 2021;13:47.
5. Madry C, Kyrargyri V, Arancibia-Cárcamo IL, et al. Microglial Ramification, Surveillance, and Interleukin-1β Release Are Regulated by the Two-Pore Domain K+ Channel THIK-1. Neuron 2018;97:299-312.e6.
6. Lou N, Takano T, Pei Y, et al. Purinergic receptor P2RY12-dependent microglial closure of the injured blood-brain barrier. Proc Natl Acad Sci U S A 2016;113:1074-9.
7. Qin C, Zhou LQ, Ma XT, et al. Dual Functions of Microglia in Ischemic Stroke. Neurosci Bull 2019;35:921-33.
8. Franke M, Bieber M, Kraft P, et al. The NLRP3 inflammasome drives inflammation in ischemia/reperfusion injury after transient middle cerebral artery occlusion in mice. Brain Behav Immun 2021;92:223-33.
9. Li Z, Song Y, He T, et al. M2 microglial small extracellular vesicles reduce glial scar formation via the miR-124/STAT3 pathway after ischemic stroke in mice. Theranostics 2021;11:1232-48.
10. Quintanilla M, Montero-Montero L, Renart J, et al. Podoplanin in Inflammation and Cancer. Int J Mol Sci 2019;20:707.
11. Noack M, Ndongo-Thiam N, Miossec P. Interaction among activated lymphocytes and mesenchymal cells through podoplanin is critical for a high IL-17 secretion. Arthritis Res Ther 2016;18:148.
12. Cimini M, Garikipati VNS, de Lucia C, et al. Podoplanin neutralization improves cardiac remodeling and function after acute myocardial infarction. JCI Insight 2019;5:126967.
13. Fei M, Wang H, Zhou M, et al. Podoplanin influences the inflammatory phenotypes and mobility of microglia in traumatic brain injury. Biochem Biophys Res Commun 2020;523:361-7.
14. Meng D, Ma X, Li H, et al. A Role of the Podoplanin-CLEC-2 Axis in Promoting Inflammatory Response After Ischemic Stroke in Mice. Neurotox Res 2021;39:477-88.
15. Wang G, Wang T, Zhang Y, et al. Schizandrin Protects against OGD/R-Induced Neuronal Injury by Suppressing Autophagy: Involvement of the AMPK/mTOR Pathway. Molecules 2019;24:3624.
16. Fischer L, Rappsilber J. False discovery rate estimation and heterobifunctional cross-linkers. PLoS One 2018;13:e0196672.
17. David CC, Jacobs DJ. Principal component analysis: a method for determining the essential dynamics of proteins. Methods Mol Biol 2014;1084:193-226.
18. Al Mamun A, Chauhan A, Qi S, et al. Microglial IRF5-IRF4 regulatory axis regulates neuroinflammation after cerebral ischemia and impacts stroke outcomes. Proc Natl Acad Sci U S A 2020;117:1742-52.
19. Li L, Qin JJ, Guo S, et al. Attenuation of cerebral ischemic injury in interferon regulatory factor 3-deficient rat. J Neurochem 2016;136:871-83.
20. McDonough A, Lee RV, Noor S, et al. Ischemia/Reperfusion Induces Interferon-Stimulated Gene Expression in Microglia. J Neurosci 2017;37:8292-308.
21. Liao Y, Cheng J, Kong X, et al. HDAC3 inhibition ameliorates ischemia/reperfusion-induced brain injury by regulating the microglial cGAS-STING pathway. Theranostics 2020;10:9644-62.
22. Popiolek-Barczyk K, Ciechanowska A, Ciapała K, et al. The CCL2/CCL7/CCL12/CCR2 pathway is substantially and persistently upregulated in mice after traumatic brain injury, and CCL2 modulates the complement system in microglia. Mol Cell Probes 2020;54:101671.
23. Lin W, Wang N, Zhou K, et al. RKIP mediates autoimmune inflammation by positively regulating IL-17R signaling. EMBO Rep 2019;20:e47502.
24. Noack M, Ndongo-Thiam N, Miossec P. Role of podoplanin in the high interleukin-17A secretion resulting from interactions between activated lymphocytes and psoriatic skin-derived mesenchymal cells. Clin Exp

Immunol 2016;186:64-74.
25. Severinova E, Alikunju S, Deng W, et al. Glucocorticoid Receptor-Binding and Transcriptome Signature in Cardiomyocytes. J Am Heart Assoc 2019;8:e011484.
26. Rothe T, Ipseiz N, Faas M, et al. The Nuclear Receptor Nr4a1 Acts as a Microglia Rheostat and Serves as a Therapeutic Target in Autoimmune-Driven Central Nervous System Inflammation. J Immunol 2017;198:3878-85.
27. Wu X, Fu S, Liu Y, et al. NDP-MSH binding melanocortin-1 receptor ameliorates neuroinflammation and BBB disruption through CREB/Nr4a1/NF-κB pathway after intracerebral hemorrhage in mice. J Neuroinflammation 2019;16:192.
28. Gibson CJ, Hossain MM, Richardson JR, et al. Inflammatory regulation of ATP binding cassette efflux transporter expression and function in microglia. J Pharmacol Exp Ther 2012;343:650-60.
29. Yu Q, Zhao T, Liu M, et al. Targeting NLRP3 Inflammasome in Translational Treatment of Nervous System Diseases: An Update. Front Pharmacol 2021;12:707696.
30. Li N, Zhou H, Wu H, et al. STING-IRF3 contributes to lipopolysaccharide-induced cardiac dysfunction, inflammation, apoptosis and pyroptosis by activating NLRP3. Redox Biol 2019;24:101215.
31. Taffoni C, Steer A, Marines J, et al. Nucleic Acid Immunity and DNA Damage Response: New Friends and Old Foes. Front Immunol 2021;12:660560.
32. Wang W, Hu D, Wu C, et al. STING promotes NLRP3 localization in ER and facilitates NLRP3 deubiquitination to activate the inflammasome upon HSV-1 infection. PLoS Pathog 2020;16:e1008335.

(English Language Editor: L. Huleatt)

Cite this article as: Qian S, Qian L, Yang Y, Cui J, Zhao Y. Transcriptome sequencing analysis revealed the molecular mechanism of podoplanin neutralization inhibiting ischemia/reperfusion-induced microglial activation. Ann Transl Med 2022;10(11):638. doi: 10.21037/atm-22-1952

